Concentration and pH Dependent Aggregation of Hydrophobic Drug Molecules and Relevance to Oral Bioavailability

Yulia Volovik Frenkel,[‡] Arthur D. Clark, Jr.,[‡] Kalyan Das,[‡] Yuh-Hwa Wang,[§] Paul J. Lewi,[⊥] Paul A. J. Janssen,[⊥,†] and Eddy Arnold*[,‡]

Center for Advanced Biotechnology and Medicine and Department of Chemistry and Chemical Biology, Rutgers University, 679 Hoes Lane, Piscataway, New Jersey 08854, Department of Biochemistry and Molecular Biology, University of Medicine and Dentistry, 675 Hoes Lane, Piscataway, New Jersey 08854, and Center for Molecular Design, Janssen Pharmaceutica NV, Antwerpsesteenweg, 37, B2350 Vosselaar, Belgium

Received July 15, 2004

We have examined selected physicochemical properties of compounds from the diaryltriazine/diarylpyrimidine (DATA/DAPY) classes of non-nucleoside reverse transcriptase inhibitors (NNRTIs) and explored possible correlations with their bioavailability. In simple aqueous solutions designed to mimic the gastrointestinal (GI) environment of a fasting individual, all NNRTIs demonstrated formation of aggregates as detected by dynamic light scattering and electron microscopy. Under various conditions mimicking physiological transitions in the GI environment, aggregate size distributions were shown to depend on compound concentration and pH. NNRTIs with good absorption were capable of forming aggregates with hydrodynamic radii of ≤100 nm at higher concentrations and over wide ranges of pH, while poorly absorbed inhibitors form aggregates with radii of ≥250 nm at concentrations above 0.01 mM, probably representing precipitate. We propose a model in which the uptake rate into systemic circulation depends on having hydrophobic drug aggregates of appropriate size available for absorption at different locations within the GI tract.

Introduction

Bioavailability is a primary pharmacokinetic parameter in determining the potential success of a drug.[1] Oral bioavailability is defined as the rate and extent of drug molecule absorption into systemic circulation from the gastrointestinal (GI) tract and is governed by the drug and dosage form.[2−4] Approximately 40% of drug candidates tested in late-stage clinical trials fail because of low efficacy for reasons including poor bioavailability that can be caused by ineffective intestinal absorption and/or undesirable metabolic activity.[4−6] Reliable bioavailability evaluations generally involve testing in animal models and in human subjects, requiring considerable time and expense.[7] In vivo systems for bioavailability estimation include monitoring of drug concentrations following intraduodenal dosing in animal models (usually rat or dog) and intestinal perfusion studies in both animals and human subjects.[2,3] In vitro test formats include (1) Caco-2 cell monolayers for measurement of compound diffusion rate,[8−10] (2) intestinal tissue for permeation measurements,[11,12] and (3) immobilized artificial membrane (IAM) chromatography.[13] A number of high-throughput in vitro methods have been designed; however, they are still several orders of magnitude slower than desired and have other limitations as well.[6−8,10,14,15]

Many efforts have been made to correlate bioavailability with chemical properties of inhibitors including solubility, lipophilicity, molecular weight, and ionizability. Many potent inhibitors have been identified that are highly hydrophobic and poorly water-soluble. In the widely used biopharmaceutics drug classification system (BCS) highly hydrophobic compounds fall into low solubility high/low permeability classes II and IV.[16,17] As reviewed by Chen et al., absorption of lipophilic particles into systemic circulation occurs in a number of ways with some passing through enterocytes via paracellular and/or transcellular routes and with others through the microvilli (M) cells in Peyer's patches of mucosa-associated lymphoid tissue (MALT) in intestinal lumen via transcytosis.[18−21] Size exclusion,[22,23] dissolution,[24] transfer,[25] chylomicron,[26,27] and surface dependent[28] models for absorption of lipophilic drugs address the multidimensionality of this issue, but the lack of universality of these models suggests the need for further investigation in this field.

Non-nucleoside reverse transcriptase inhibitors (NNRTIs) belong to a class of anti-AIDS drugs that target the reverse transcriptase (RT) enzyme of HIV-1. NNRTIs tend to be highly hydrophobic and weakly ionizable compounds with molecular weights ranging from 300 to 500 Da. NNRTIs bind to a specific hydrophobic pocket in HIV-1 RT.[29−32] At present, three NNRTIs are FDA-approved drugs for treating HIV-1 infected patients. A major hurdle in designing effective NNRTIs is to overcome the effect of drug resistance. A multidisciplinary effort[33] has led to the discovery of the diaryltriazine (DATA)[34] and diarylpyrimidine (DAPY)[35] classes of NNRTIs that are highly potent against a wide range of HIV-1 resistant viral strains when tested in recombinant virus assays and in clinical trials.[33,36−38]

Some of the extremely hydrophobic and potent NNRTIs developed in our multidisciplinary design program

* To whom correspondence should be addressed. Phone: 732-235-5323. Fax: 732-235-5669. E-mail: arnold@cabm.rutgers.edu.
‡ Rutgers University.
§ University of Medicine and Dentistry.
⊥ Janssen Pharmaceutica NV.
† Deceased.

10.1021/jm049439i CCC: $30.25
Published on Web 02/26/2005

were found to be highly bioavailable in animal models and human subjects.[33,39] From studies with thousands of NNRTIs having diverse chemical structures, Dr. Paul Janssen observed that in a standard cell culture assay the maximum potency for 50% inhibition of HIV replication by NNRTIs from different chemical classes was consistently ~0.1 nM. From a consideration of the stoichiometry of inhibitor molecules per cell in culture, Janssen reasoned that the inhibitors may enter infected cells as aggregates containing hundreds of thousands of inhibitor molecules. In the current study, we examined the physicochemical properties of the DATA/DAPY classes of NNRTIs and explored possible correlations with their absorption. In simple aqueous solutions designed to mimic the gastrointestinal environment of a fasting individual, the NNRTIs demonstrated formation of aggregates as detected by dynamic light scattering (DLS). These findings provided the initial experimental support for a prediction by Dr. Janssen that the hydrophobic NNRTIs would form aggregates in aqueous solution with sizes appropriate for absorption into the lymphatic system.[33,39] Analysis of aggregate size distributions under various physiological conditions demonstrated dependence of aggregation behavior on compound concentration and solution pH. Our data also suggested correlation of aggregate size with drug absorption data obtained from animal models and human clinical trials. On the basis of our observations, we have established a potential in vitro/in vivo correlation assay for highly hydrophobic drug candidates such as NNRTIs and propose a possible model for a location and aggregate size dependent absorption pathway for transport of hydrophobic drugs into lymphatic circulation from the GI tract. An effective in vitro/in vivo correlation assay for BCS classes II and IV compounds, in conjunction with other physicochemical, cell-based, and computational techniques,[40] may lead to more reliable bioavailability assessment methods for hydrophobic compounds at the early stages of drug development.

Materials and Methods

Dynamic Light Scattering (DLS). Data collection was performed using the DynaPro-MS800 dynamic light scattering/molecular sizing instrument[41] with argon laser wavelength λ = 830 nm, a detector angle of 90°, and typical sample volume of 20 μL. Each light scattering experiment consisted of 20 or more independent readings, each 10 s in duration. Data analysis was conducted using DynaPro Instrument Control Software for Molecular Research DYNAMICS (version 5.26.60). For very large particles with radii greater than 250 nm, full data collection was unfeasible; therefore, less than 20 measurements were acquired and size determination was based on empirical data readings. Each DLS experiment was repeated in triplicate. To minimize dust interference in light scattering experiments, all stock solutions were filtered with 0.22 μm MillexGV sterile filters.

All NNRTIs were dissolved in 100% DMSO, and stock solutions at 50 or 20 mM concentrations were kept frozen at −80 °C. Inhibitors were diluted from DMSO stocks into solutions mimicking GI conditions of a fasting individual, vortexed for at least 10 s, and then evaluated by DLS. Gastric conditions in vitro were simulated by using (a) 0.15 M HCl, pH 1.5, (b) 0.15 M HCl, pH 1.5 with 0.1% (v/v) tyloxapol (surfactant), and (c) 20 mM malonic acid, pH 1.5. Note that although the 0.15 M HCl, pH 1.5 condition showed formation of NNRTI aggregates, it was a highly unstable system for DLS evaluation and therefore was replaced with 20 mM malonic acid buffer at pH 1.5, which produced aggregates of similar size, gave more stable DLS readings, and permitted buffering in relevant pH ranges. The solutions intended to mimic pH transitions in the GI tract were 20 mM malonic acid for pH ranging from 1.5 to 4.5 and 50 mM malonic acid for pH ranging from 5.5 to 6.5.

Preliminary analysis of NNRTI aggregation at 25 and 37 °C was conducted using five NNRTI compounds and showed that temperature change had only a modest effect on the size distribution of NNRTI aggregates in 0.15 M HCl with and without surfactant (data not shown). Therefore, the temperature was kept at 25 °C for all subsequent DLS measurements.

Transmission Electron Microscopy (TEM). Inhibitors were diluted from 20 or 50 mM stocks into 0.15 M HCl, pH 1.5, with and without 0.1% tyloxapol to various concentrations: 0.1, 0.25, 0.5, and 1 mM. At room temperature, 5 μL samples of the reaction mixtures were applied to the carbon-coated grids and negatively stained with 2% uranyl acetate. Micrographs were taken on a JEOL 1200 EX transmission electron microscope at 80 kV.

Results

Aggregation behavior of NNRTIs was examined as a function of concentration and pH using dynamic light scattering (DLS) and electron microscopy (EM). A total of 36 DATA/DAPY NNRTIs were used in the DLS analysis, and three compounds were evaluated by EM. Of the 36 NNRTIs, 15 compounds had known animal (rat and dog) absorption and, in six cases, human absorption (see Table 1, Figure 1). The absorption of a drug molecule, which is determined as the exposure or area under the curve (AUC) of the plasma concentration curve as a function of time following oral administration, has been used in this study as a correlate of oral bioavailability. The rat and human absorption data for DATA/DAPY NNRTIs were shown to correlate better than dog and human absorption data.[39] Therefore, only rat and human absorption data were used to search for correlations with DLS and EM findings. Compounds with the highest exposure in the rat were **10**, **8**, and **15** (Table 1). In human subjects the same three compounds were highly bioavailable. In addition to analyzing rat and human exposure data, Lewi et al. also characterized NNRTIs in terms of pK_a, ClogP, and other experimental and computed physicochemical parameters.

Compounds with Good and Poor Absorption Show Distinct Aggregation Behavior. DLS analysis of 36 NNRTIs detected the presence of aggregate species in simulated gastric solutions, both in the presence and in the absence of surfactant in DMSO and in formulation-mimicking conditions (Figure 2). Surfactants such as tyloxapol were initially introduced into the system in an attempt to stabilize the DLS measurements, which were erratic presumably because of rapid changes in the sizes of the drug aggregates. A series of nonionic detergents including β-octylglucoside, Triton X-100, and tyloxapol were tested for their ability to stabilize the DLS measurements (data not shown), and tyloxapol was found to have the most favorable effect in terms of stabilization together with forming relatively uniform detergent micelles at a size easily distinguishable from the drug aggregates. In comparison to results obtained in the absence of detergent, an ~20 nm increase in the average hydrodynamic radii of the aggregated species for compounds from the good absorption group and a significant decrease in size for one compound from the poor absorption group were observed in the presence of surfactant (parts B and C of Figure 2). Another additive

Table 1. Absorption, pK_a, ClogP, and R_h Data for 15 NNRTIs[a]

compd	ID/generic name	AUC rat (μg·h/mL)	AUC human (μg·h/mL)	pK_a	ClogP	$R_{h,+s}$ (nm)	SD (nm)	$R_{h,-s}$ (nm)	SD (nm)
1	R106168	1.5		3.1	4.7	69.5	11.7	54.0	4.6
2	R120393	67.5		3.3	4.2	96.0	15.1	70.0	1.1
3	R124043	4.4		2.8	5.3	101.3	63.0	82.2	12.4
4	R126874	7.3			5.5	99.8	36.0	75.0	4.1
5	R129385	0.6		1.9	4.3	>250.0	na	>250.0	na
6	R132914	0.1	0.1	2.5	4.7	52.0	10.6	33.6	22.6
7	R138750	5.2	0.7	3.8	5.6	90.6	30.6	73.3	1.1
8	R147681/TMC120/dapivirine	19.4	4.7	5.8	6.3	94.8	16.7	66.2	3.9
9	R152649	8.4		2.6	5.5	82.6	4.0	55.3	0.9
10	R152929	49.3	8.2	5.1	5.3	80.6	22.0	67.6	11.3
11	R156204	6.8	0.9	3.6	7	71.4	28.2	50.4	5.7
12	R157753	0.1		2.7	5.2	34.2	5.1	>250.0	na
13	R165335/TMC125/etravirine	0.6	0.4	3.5	5.2	>250.0	na	>250.0	na
14	R185545	0.6		2.0	4.1	>250.0	na	>250.0	na
15	R278474/TMC278/rilpivirine	9.8		5.6	5.8	52.5	6.0	35.6	18.0

[a] Rat and human absorption (exposure, AUC) values were determined following oral administration of 40 and 100 mg/kg doses, respectively.[39] $R_{h,+s}$ and $R_{h,-s}$ are average values for hydrodynamic radii (R_h) measured with and without surfactant, respectively. The averages and standard deviations (SD) were calculated on the basis of four independent measurements for each inhibitor (see details in Materials and Methods). $R_{h,+s}$ measurements were collected in 0.15 M HCl, 0.1% tyloxapol, pH 1.5, and $R_{h,-s}$ measurements were collected in 20 mM malonic acid, pH 1.5.

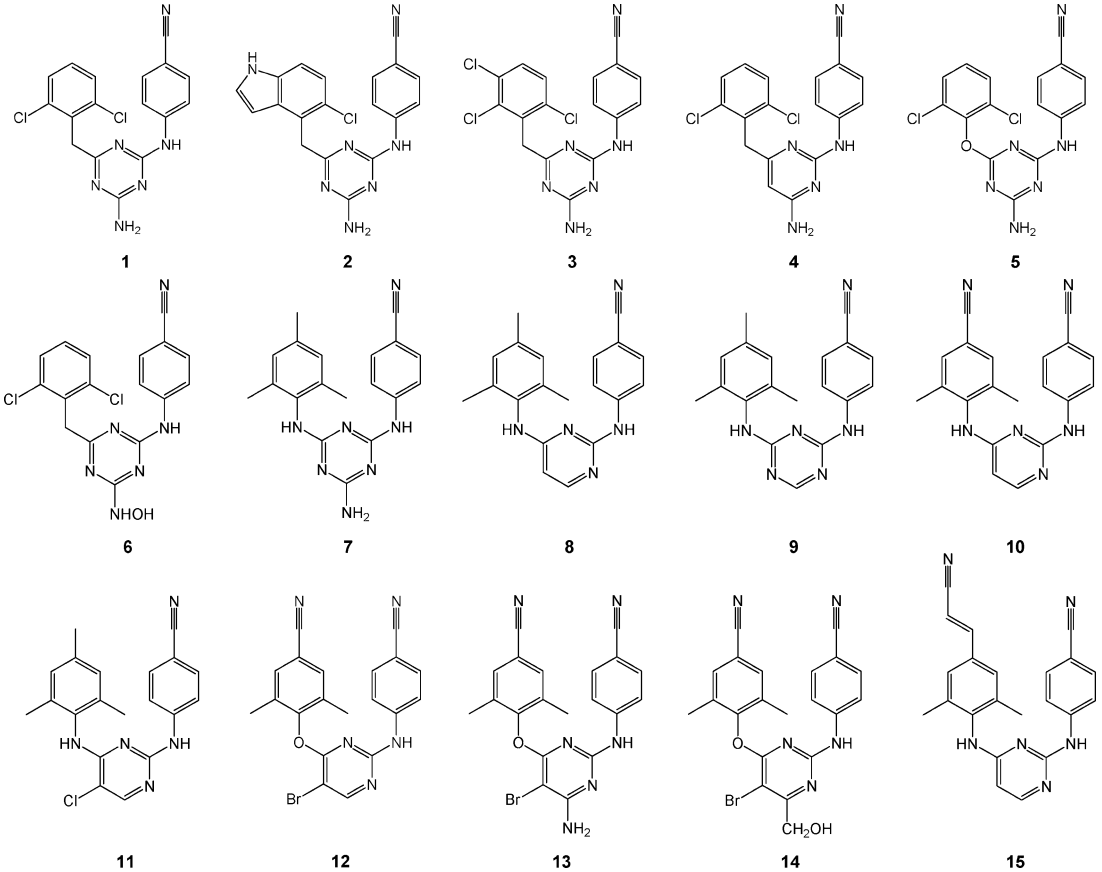

Figure 1. Chemical structures of NNRTIs used in the study.

in the experimental system was DMSO, present in final solutions at 0.2% (v/v). DLS evaluation of these solutions containing DMSO without drug did not show the presence of aggregate structures. Also, in a study in which DMSO was replaced by a formulation-mimicking condition containing PEG400, it was also observed that drug aggregate formation did not depend on the presence of DMSO (data not shown).

Although all NNRTIs showed aggregation, the aggregate sizes varied for different compounds. As shown in Figure 2A, the measured aggregate sizes fell into two distinct groups. One group of compounds had aggregate radii ranging from 30 to 110 nm, while the measured radii in the other group were greater than 250 nm. Analysis of hydrodynamic radii (R_h) measured by DLS using various gastric-mimicking conditions for 15 NNRTIs with known absorption revealed that compounds with more favorable absorption belonged to the group with an aggregate size ranging from 30 to 100 nm (see parts B and C of Figure 2 and Table 1) while compounds with aggregate radii greater than 250 nm invariably had poor absorption (AUC < 1.0 μg·h/mL in the rat). From these data, the success of in vitro/in vivo classification of favorable versus poor absorption group based on

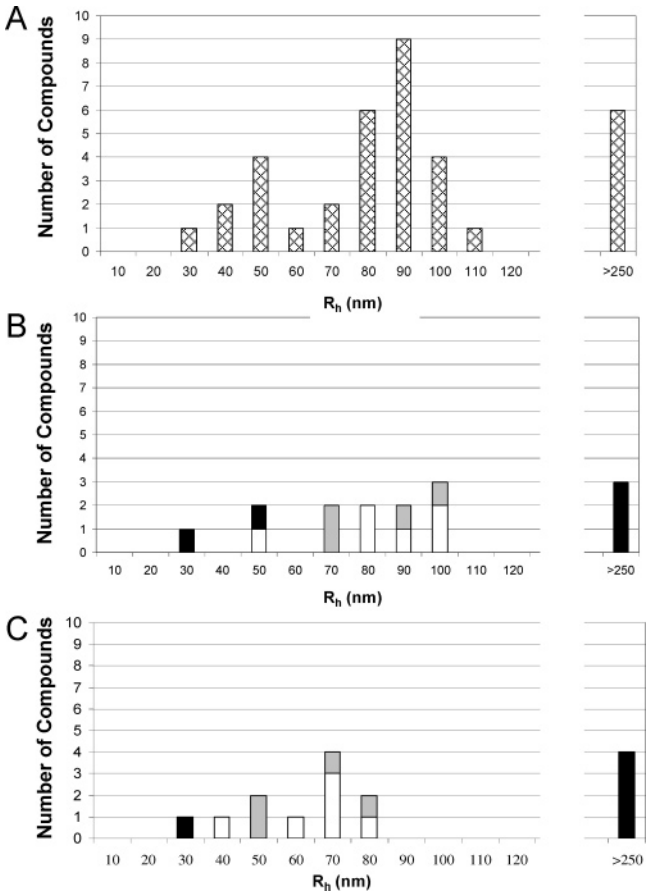

Figure 2. Aggregate size distribution plots. (A) Size distribution of aggregates is expressed as the number of compounds forming particles with mean hydrodynamic radii (R_h) as determined using dynamic light scattering (DLS) for 36 NNRTIs at 0.1 mM concentration in simple stomach-mimicking solutions (0.15 M HCl, pH 1.5, with and without stabilizing agent tyloxapol). NNRTI aggregate sizes fell into two groups: (1) radii ranging from 30 to 110 nm and (2) radii greater than or equal to 250 nm. (B) DLS measurements for 15 compounds are shown with known absorption using the same conditions as (A). Assignments are as follows: white, good absorption (AUC rat/human > 5 μg·h/mL); gray, intermediate absorption (1 μg·h/mL < AUC in rat/human < 5 μg·h/mL); black, poor absorption (AUC in rat/human < 1 μg·h/mL). (C) Results from DLS analysis of the same compounds as in (B) are shown for a different gastric-mimicking condition (20 mM malonic acid, pH 1.5). Assignments are the same as in (B).

aggregation behavior was determined to be 86.7% for 0.15 mM HCl with surfactant at pH 1.5 (13 of 15 assigned correctly to absorption group) and 93.3% for 20 mM malonic acid without surfactant at pH 1.5 (14 of 15 correctly assigned). On the basis of Fisher's exact test,[42] the two-tailed probability for the 2 × 2 aggregation/exposure table is 0.004. The overall prediction accuracy of absorption and probably bioavailability was better in the absence of the surfactant. Nonetheless, it must be stressed that the presence of the surfactant seemed to facilitate transition of compounds with poor absorption from precipitated to aggregated states, which suggests that including this type of excipient in oral formulations could be favorable.

In addition to the aggregate size distributions, we also looked at the heterogeneity of aggregate populations for different NNRTIs. In Figure 3, we compared the aggregate size distributions for two NNRTIs, **15** and **8** (both at 0.1 mM), against the blank of the gastric solution in which these NNRTIs were dissolved (0.15 M HCl with 0.1% surfactant). Note that tyloxapol alone, the nonionic surfactant used in this study, formed small micelles in the aqueous solutions with R_h = 3.5 nm.[43] Plots of percent intensity and mass generated by the DynaPro software package (Figure 3A) indicated the presence of two aggregate populations corresponding to surfactant micelles (R_h = 3.5±0.3 nm) and drug aggregate species. Typical individual experimental DLS evaluations of compounds **15** and **8** in the presence of tyloxapol are shown in Figure 3A. Their radii were determined to be 44 and 87 nm, respectively, based on percent mass calculations, with compound **15** forming smaller aggregates with a size distribution somewhat narrower than that of compound **8**. Aggregate populations were also studied by EM and visualized by negative staining with uranyl acetate (Figure 3B). When prepared using 0.25 mM drug concentrations, the EM images showed the presence of spherical particles (Figure 3B). Compound **15** aggregates were smaller and more consistent in size, with average radii measured from the EM images of around 30 ± 10 nm versus 50 ± 30 nm for compound **8**. The differences between EM and DLS size estimates may have been due to differences in specimen preparation.

Different Concentration and pH Dependent Aggregation Behavior of Compounds with Good and Poor Absorption. To investigate the possible dependence of NNRTI aggregation on concentration and pH, we generated a dilution series from 10 to 0.001 mM in the physiologically relevant pH range from 1.5 to 6.5. On the basis of our results, all aggregate sizes for NNRTIs increased with increasing compound concentration. As an example of concentration dependent behavior, EM images of compound **15** at 0.25 and 0.5 mM concentrations are presented in Figure 4A. The 2-fold increase in concentration led to an increase in aggregate radii from ~30 to ~60 nm. At the higher concentration aggregates coalesced into very large structures. However, even at the higher compound concentration a minority of small aggregates were present.

The effect of pH variation on the size distribution of NNRTI aggregates was evaluated for three compounds (**5**, **10**, and **11**) with different rat/human absorption (Table 1). On the basis of DLS analysis, the pH dependence of particle size distribution for all three compounds at 0.1 mM was reflected in an increase in aggregate size with increasing pH (Figure 4B). Compound **10** was the most bioavailable inhibitor of the three compared, and its aggregation behavior was least affected by changes in pH, with aggregate radii below 50 nm until pH reached 4.5, while compound **5** formed aggregates with radii greater than 200 nm at pH values 2.5 and above. Compound **5** had the most pH-sensitive aggregation behavior and was the least bioavailable of the three compounds. Compound **5** was classified as poorly bioavailable on the basis of oral administration studies (see Table 1); when compared to compounds with better absorption, the behavior of **5** was distinct because it was highly susceptible to formation of large structures at pH values above 1.5, while with compounds with

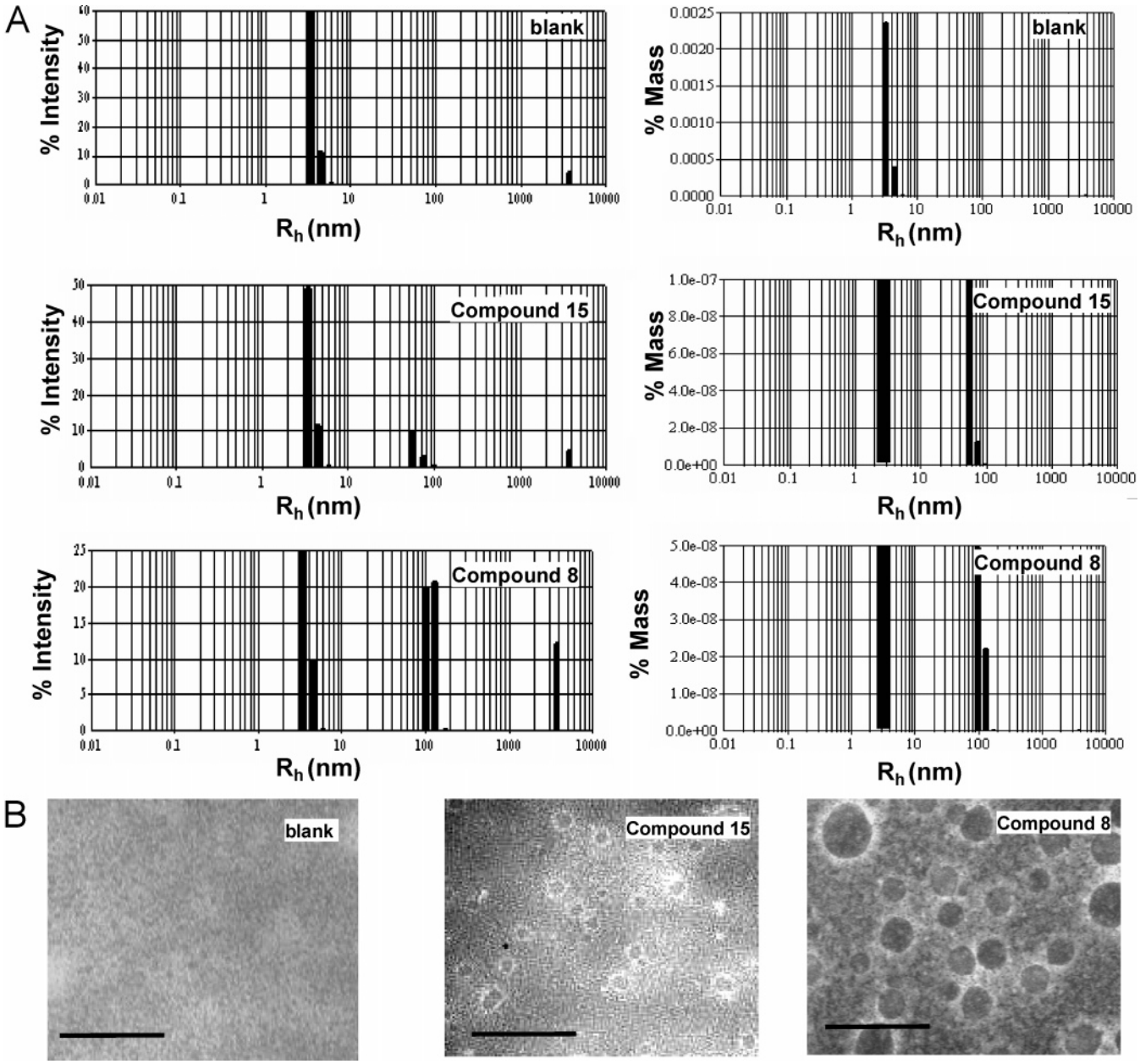

Figure 3. Dynamic light scattering and electron miscroscopy. (A) Shown are DLS % intensity and % mass versus R_h histograms for solution without drug (blank) and the same containing 0.1 mM compound **15** and 0.1 mM compound **8**. The blank contains 0.1% tyloxapol in 0.15 M HCl, pH 1.5. The aggregate populations at 3.5 nm radii correspond to tyloxapol micelles. The peaks at ~3000 nm correspond to instrumental artifacts due to a small amount of background scattering. (B) Shown are electron micrographs of blank, 0.25 mM compound **15**, and 0.25 mM compound **8**. The black bar corresponds to 200 nm. The blank solution is the same as in (A).

better absorption such as **10** and **11**, the aggregate sizes increased more gradually with increasing pH.

After studying aggregation as a function of concentration and pH as single variables, we investigated the combinatorial effects of these parameters on the aggregation of NNRTIs with different rat/human absorption properties (Figure 4C). Compounds **10**, **11**, and **5** were considered to have good, intermediate, and poor absorption, respectively, in rats and human subjects (Table 1). While all compounds formed large structures, possibly representing precipitate, at higher concentrations and solution pH values, the data indicated that compounds with good or intermediate absorption formed smaller aggregates (30 nm < R_h < 100 nm) at higher concentrations and pH while those with poor absorption formed larger structures. Also, as evident from the graphs in Figure 4C, there was a concentration dependent threshold around 0.01 mM below which all studied compounds formed aggregates with R_h values below 50 nm.

Structural and Mechanistic Considerations for Aggregate Formation. A number of structure−activity trends could be discerned between the molecular structures of selected NNRTIs and their ability to form aggregate structures with radii of 30−100 nm. In the series of 15 DATA/DAPY NNRTIs studied, the five molecules that contain oxygen atoms (either as aryl ring linkers or as hydroxyl substituents) had the lowest exposures in rat (compounds **5**, **6**, **12**−**14**; see Table 1) and four of the five formed larger structures (R_h > 250

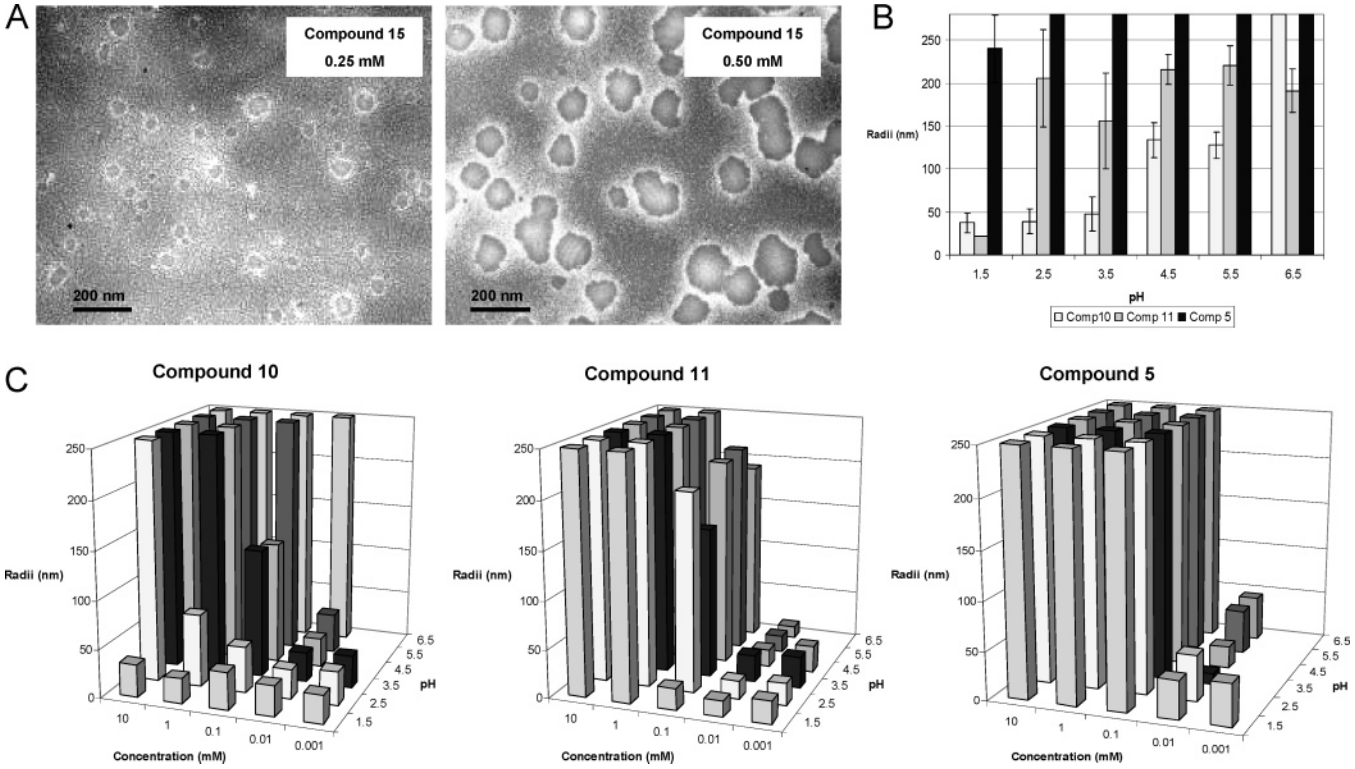

Figure 4. Concentration and pH dependence of aggregate sizes (RCpH plots): (A) concentration dependent aggregation size distribution visualized by EM for compound **15** at 0.25 and 0.50 mM concentrations; (B) pH dependent size distribution for compounds (at 0.1 mM) with different bioavailabilities. Assignments are as follows: white, good absorption (AUC rat/human > 5 μg·h/mL); gray, intermediate absorption (1 μg·h/mL < AUC in rat/human < 5 μg·h/mL); black, poor absorption (AUC in rat/human < 1 μg·h/mL). (C) RCpH plots illustrate the combinatorial effects of concentration and pH changes on aggregate size distribution for compounds with different bioavailabilities. The readings below 0.001 mM were not reproducible because of instrument limitations.

nm) in the pH 1.5 malonate buffer condition, as opposed to the other 10 that in each case formed aggregate structures with radii of 30−100 nm. These oxygen atoms are able to act as hydrogen-bond acceptors even at pH 1.5, allowing for contact patterns different from those of nitrogen or carbon atoms. Also, some trends could be seen relating the compound pK_a values and aggregation:[39] the three DAPY derivatives with the three highest pK_a values (pK_a > 5; compounds **8**, **10**, and **15**) formed aggregates and had very good rat and human absorption. The five compounds with the lowest rat AUC values all had pK_a values 3.5 or lower, and as stated above, four of the five formed larger structures in the malonate, pH experiments (Table 1 and Figure 2C). Given the hints from EM that larger structures might form from the coalescence of smaller aggregates, these data may imply that the higher pK_a values, which would correspond to more complete ionization (by protonation of pyrimidine nitrogens in this case), might permit stabilization of the aggregates with radii of 30−100 nm under acidic conditions that may be important for efficient absorption after oral administration. These observations are confined to the DATA/DAPY series studied in this work, and different classes of hydrophobic compounds are expected to have their own structure−aggregation correlations.

Although the precise mechanism of aggregate formation is unknown to us, we expect that the process is driven, among other not yet identified factors, by burial of the hydrophobic surface area of the compounds (as with the hydrophobic effect in the formation of oil droplets in water or the folding of proteins in aqueous environments), which may be balanced by the energy cost incurred by forming cavities in the water. The arrangement of molecules within the aggregates may resemble an environment anywhere along the continuum from liquid-like to liquid crystals to solid-like in which microcrystalline domains may be present. The ways in which the hydrophobic molecules will pack in the aggregates will depend on solution conditions (pH, buffer, salt, ionic strength, etc.) and the detailed structures and properties of the molecules, including the number of polar atoms, number of hydrogen bond donors and acceptors, conformational flexibility, and presence of ionized groups, among other factors. Depending on the solvent, salts, and other additives (e.g., tyloxapol or PEG400) in solution, additional molecules and species may be present within the aggregates.

Discussion

Janssen's Hypothesis: Hydrophobic Drugs May Be Taken Up as Aggregates. After working for many years with about 4000 NNRTIs, Dr. Paul Janssen and his colleagues at the Janssen Center for Molecular Design formulated a hypothesis and proposed a possible model of oral absorption for highly hydrophobic/lipophilic compounds. Even with the most potent NNRTIs there seemed to be a threshold minimum EC_{50} value of ~0.1 nM in a standard cell-based assay.[44] On the basis of this observation, Dr. Janssen hypothesized that NNRTIs were absorbed as aggregates as opposed to individual molecules. By calculation of the number of

molecules per cell from the EC_{50} threshold value and the number of cells in the cell culture experiments, it could be estimated that the aggregates would contain $\sim 2 \times 10^6$ NNRTI molecules (with an average molecular volume of 0.38 nm^3 for a typical NNRTI) and would have a radius of ~57 nm. Assuming that the volume and the mass of different NNRTI molecules vary, the particles were predicted to form aggregates with diameters ranging from approximately 50 to 70 nm. Concurrent studies conducted in dog models showed that high concentrations of orally administered NNRTIs were present in lymph tissue during the early phase of absorption (up to ~4 h) followed by equilibration (after ~6 h) between lymph and plasma concentrations. Building on these findings, the aggregation theory stated earlier was extended to a lymphatic absorption of aggregates model in which orally administered NNRTIs may form aggregates in the GI tract where they can be absorbed by M cells of Peyer's patches of MALT and then drained into lymphatic circulation and emptied into the systemic compartment.[39]

Aggregation and Absorption of NNRTIs. The physicochemical properties of hydrophobic compounds evaluated in this study displayed behavior consistent with Dr. Paul Janssen's hypothesis and offered support for the prediction that the presence of the NNRTI aggregates favors their lymphatic absorption via M cells in MALT of the GI tract. As has been established by Dressman et al., poorly soluble compounds (such as in BCS classes II and IV) have dissolution rate-limiting absorption profiles that can be affected by the GI tract environment.[4,24,45] It has also been proposed that solubility plays a crucial role in hydrophobic drug absorption rate. A transfer model has been proposed suggesting that high drug concentrations can lead to precipitation during transit across the pH gradient of the GI tract that can be correlated with poor oral absorption.[25,46] Lymphatic absorption of drug molecules is not a new concept; however, the mode of transport proposed in our model is. Most lymphatic drug absorption paradigms described to date are based on the ability of lipophilic drugs to solubilize in the chylomicron fraction of the lymph.[26,27] Our model suggests a parallel mode of absorption that is specific to those lipophilic drugs, such as the NNRTIs studied here, that have the ability to form small aggregated structures independent of either natural triglycerides or formulation additives acting as lipid vehicles. During the course of this study, a number of reports have appeared documenting that hydrophobic drug candidates can form aggregates in aqueous solutions.[47−50] McGovern et al. established that the aggregation behavior of hydrophobic drugs was responsible for promiscuous behavior in high-throughput screening for new lead compounds. It was proposed that hydrophobic compounds form aggregates capable of reversibly sequestering proteins in a nonspecific manner leading to spurious identification of active inhibitors (hits) in high-throughput assays.[48] In our work we independently developed DLS and EM analytical methods to evaluate hydrophobic aggregation behavior of NNRTIs in GI tract mimicking conditions. In this work we have also developed a model that integrates the available information to explain the unique absorption properties of highly hydrophobic compounds.

For the NNRTIs used in our study, oral bioavailability in human subjects was established by administration of 100 mg doses and determination of corresponding absorption (AUC) values. Assuming an immediate release formulation in a fasting individual and stomach volume in the range of 50−250 mL, the approximate gastric concentration of NNRTIs with molecular masses between 300 and 500 Da can be estimated to vary roughly from 1 to 10 mM. At high drug concentration and pH, our data indicated a sharp transition from aggregates to larger structures, likely representing a phase transition to precipitate formation. It was also observed that at concentrations below 0.01 mM, compound aggregation became concentration and pH independent and the aggregate size for all compounds was consistently smaller than 100 nm in diameter (see Figure 4). In conjunction with the earlier findings by Desai et al., that polymeric particles with diameter of ~100 nm are absorbed more readily in Peyer's patches than larger particles,[23] it may be that all NNRTIs at concentrations below 0.01 mM would form aggregates of appropriate size that can be absorbed via the M cell route. In addition to this observation it should be stressed that there were also some NNRTIs that were able to form aggregates at concentrations above 0.01 mM, suggesting that those compounds could be absorbed efficiently by M cells at drug concentrations higher than 0.01 mM.

In addition to the supportive findings on the possible M cell absorption of hydrophobic inhibitor aggregates, we also observed correlations between the in vitro generated aggregation of NNRTIs and their oral bioavailability in rat and man. Under simulated gastric conditions of low pH (1.5) and drug concentrations ranging from 1 to 10 mM, inhibitors with low absorption formed large structures with radii greater than 250 nm, while compounds with better absorption formed smaller aggregates with smaller dimensions. The aggregate size and good absorption correlation did not hold true when aggregation was measured at NNRTI concentrations below 0.01 mM because all NNRTIs formed aggregates with radii equal to or less than 50 nm. On the basis of our analysis, in vivo/in vitro correlation properties for NNRTIs can be summarized by the following statement: NNRTIs capable of forming aggregates with radii less than or equal to 50 nm at concentrations above 0.01 mM, at various physiologically relevant pH points, in vitro, are more likely to have good oral bioavailability.

Location Dependent Hydrophobic Drug Absorption Model. On the basis of the aggregate lymphatic absorption model and correlations established in this study, we propose a GI location and aggregate size dependent model for absorption of hydrophobic drugs (Figure 5). The physiology of the GI tract is such that gastric absorption of many drugs is low because of the inability to cross the mucus lining of the stomach.[51] A locus of high absorption in the GI tract is at the upper small intestinal region called the duodenum. Although the duodenum is a favorable absorption site, the drug residence time in this region of the GI tract is comparably short; therefore, regions of absorption such as the colonic area, where the rate of absorption is low but the residence time is significantly longer, are of interest as

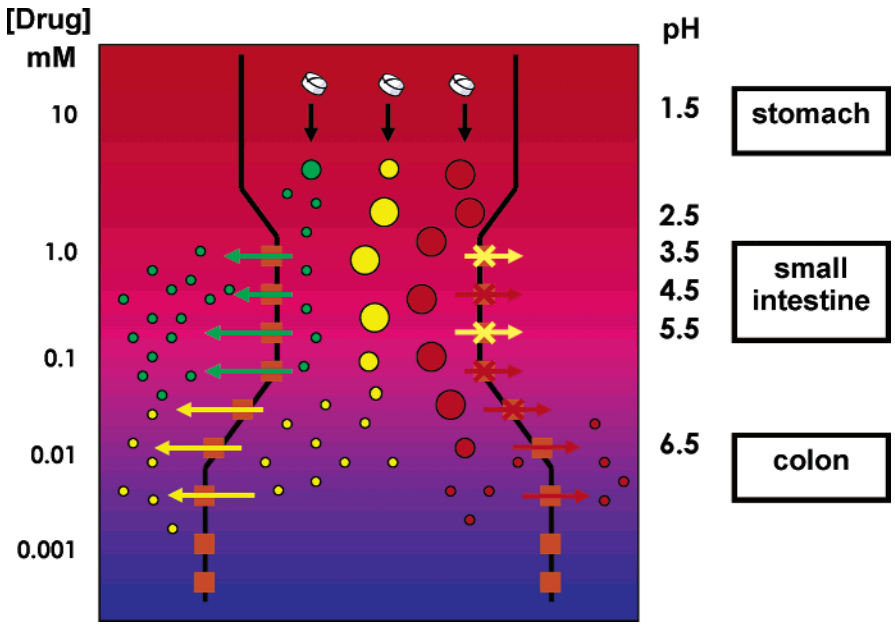

Figure 5. Location dependent hydrophobic drug absorption model. Bold lines represent the GI tract: stomach, small intestine, and colon. Orange squares represent various absorptive cells in the GI tract including M cell and enterocytes. The color gradient reflects the pH changes in respective sections of the GI (red, low pH; blue, high pH). Rough estimates of pH and concentration are shown on the right and left sides of the image, respectively. Color assignment is as follows: red, poor absorption (AUC in rat/human < 1 μg·h/mL); yellow, intermediate absorption (1 μg·h/mL < AUC in rat/human < 5 μg·h/mL); green, good absorption (AUC rat/human > 5 μg·h/mL).

well.[52,53] On the basis of our physicochemical findings, highly hydrophobic drug candidates in immediate release formulations can form aggregates in the stomach environment and some drugs can form small aggregates even at relatively high concentrations. If aggregates of the appropriate size can be maintained with increasing pH during the transition through the GI tract, larger numbers of aggregates potentially would enter the duodenum for absorption by M cells (and potentially other absorptive cells including enterocytes). Assuming that the aggregate lymphatic absorption model is correct, the presentation of a larger number of drug aggregates of appropriate size to the duodenal surface would result in high drug absorption and hence high absorption. On the other hand, compounds that are unable to form large numbers of aggregates at high drug concentrations in the stomach would miss the duodenal absorption opportunity and only at ~0.01 mM concentration and below would be able to form aggregates with radii less than 100 nm as the predominant species. Formation of aggregates for these drugs would take place at the later stages of GI transit and would result in presentation to less efficient absorption sites in the system, which could explain the low absorption properties associated with these compounds.

Conclusions

In addition to profiling the solution aggregation behavior of a series of NNRTIs, the present study provides potential templates for the development of an in vitro testing method for analysis of highly hydrophobic compounds in drug design schemes. Others have reported that several physicochemical parameters influence aggregation of lipophilic compounds. Here, we propose a model that relates aggregate radius, concentration, and pH dependence in the GI tract to oral absorption of hydrophobic drugs. Our data and observations initially established that NNRTIs can form aggregates in aqueous solution. NNRTIs with good absorption form aggregates with radii between 30 and 110 nm whose sizes are less dependent on concentration and pH changes than those with poor absorption. The current study has been done with a relatively small group of compounds. If the same pattern of behavior can be observed with a larger pool of hydrophobic drugs, this method could conceivably form the basis for a high-throughput assay at the early stages of drug development to classify which compounds are likely to have favorable or alternatively highly unfavorable absorption.

The present study has revealed correlations between the physicochemical properties and absorption of hydrophobic NNRTIs; however, these are only the initial steps toward understanding drug aggregate formation and absorption. Future research studies will be focused on understanding the phase transitions from the aggregated state to precipitate as well as the potential physiological implications of these findings. Some of the pressing questions include the following. Do aggregates form in the body? If they do, then what are their sizes and population distribution? How does aggregate formation depend on the presence of many other substances? If aggregates form in the body, then how do they get into cells and what happens to them when they are inside the cell?

Acknowledgment. We thank Hilde De Man, Walter van den Broeck, our other colleagues from CMD and Janssen Pharmaceutica, and other members of the Arnold laboratory at CABM for providing information about the compounds used for the studies and for helpful discussions. Yulia Volovik Frenkel was supported in part by a fellowship from NIH Rutgers University Training Grant in Molecular Biophysics (Grant T32 GM 08319), and the Arnold laboratory efforts were funded

by research grants from Janssen Research Foundation and NIH (R37 AI 27690 and P01 GM 66671 to E.A.). This study was inspired by hypotheses formulated by the late Dr. Paul Janssen, whose wisdom, great scientific insight, and kindness are going to be greatly missed.

References

(1) Ahr, G.; Voith, B.; Kuhlmann, J. Guidances related to bioavailability and bioequivalence: European industry perspective. *Eur. J. Drug Metab. Pharmacokinet.* **2000**, *25*, 25−27.

(2) Rosenberg, S. H.; Spina, K. P.; Condon, S. L.; Polakowski, J.; Yao, Z.; Kovar, P.; Stein, H. H.; Cohen, J.; Barlow, J. L.; Klinghofer, V.; et al. Studies directed toward the design of orally active renin inhibitors. 2. Development of the efficacious, bioavailable renin inhibitor (2*S*)-2-benzyl-3-[[(1-methylpiperazin-4-yl)sulfonyl]propionyl]-3-thiazol-4-yl-L-alanine amide of (2*S*, 3*R*,4*S*)-2-amino-1-cyclohexyl-3,4-dihydroxy-6-methylheptane (A-72517). *J. Med. Chem.* **1993**, *36*, 460−467.

(3) Rosenberg, S. H.; Spina, K. P.; Woods, K. W.; Polakowski, J.; Martin, D. L.; Yao, Z.; Stein, H. H.; Cohen, J.; Barlow, J. L.; Egan, D. A.; et al. Studies directed toward the design of orally active renin inhibitors. 1. Some factors influencing the absorption of small peptides. *J. Med. Chem.* **1993**, *36*, 449−459.

(4) Martinez, M. N.; Amidon, G. L. A mechanistic approach to understanding the factors affecting drug absorption: a review of fundamentals. *J. Clin. Pharmacol.* **2002**, *42*, 620−643.

(5) Li, A. P. Screening for human ADME/Tox drug properties in drug discovery. *Drug Discovery Today* **2001**, *6*, 357−366.

(6) Li, A. P. Advancing technologies for accelerated drug development. *Drug Discovery Today* **2003**, *8*, 200−202.

(7) White, R. E. High-throughput screening in drug metabolism and pharmacokinetic support of drug discovery. *Annu. Rev. Pharmacol. Toxicol.* **2000**, *40*, 133−157.

(8) Caldwell, G. W.; Easlick, S. M.; Gunnet, J.; Masucci, J. A.; Demarest, K. In vitro permeability of eight beta-blockers through Caco-2 monolayers utilizing liquid chromatography/electrospray ionization mass spectrometry. *J. Mass Spectrom.* **1998**, *33*, 607−614.

(9) Larger, P.; Altamura, M.; Catalioto, R. M.; Giuliani, S.; Maggi, C. A.; Valenti, C.; Triolo, A. Simultaneous LC−MS/MS determination of reference pharmaceuticals as a method for the characterization of the Caco-2 cell monolayer absorption properties. *Anal. Chem.* **2002**, *74*, 5273−5281.

(10) Fung, E. N.; Chu, I.; Li, C.; Liu, T.; Soares, A.; Morrison, R.; Nomeir, A. A. Higher-throughput screening for Caco-2 permeability utilizing a multiple sprayer liquid chromatography/tandem mass spectrometry system. *Rapid Commun. Mass Spectrom.* **2003**, *17*, 2147−2152.

(11) Yu, L. X.; Lipka, E.; Crison, J. R.; Amidon, G. L. Transport approaches to the biopharmaceutical design of oral drug delivery systems: prediction of intestinal absorption. *Adv. Drug Delivery Rev.* **1996**, *19*, 359−376.

(12) Junginger, H. E.; Hoogstraate, J. A.; Verhoef, J. C. Recent advances in buccal drug delivery and absorption—in vitro and in vivo studies. *J. Controlled Release* **1999**, *62*, 149−159.

(13) Pidgeon, C.; Ong, S.; Liu, H.; Qiu, X.; Pidgeon, M.; Dantzig, A. H.; Munroe, J.; Hornback, W. J.; Kasher, J. S.; Glunz, L.; et al. IAM chromatography: an in vitro screen for predicting drug membrane permeability. *J. Med. Chem.* **1995**, *38*, 590−594.

(14) Ungell, A. L.; Nylander, S.; Bergstrand, S.; Sjoberg, A.; Lennernas, H. Membrane transport of drugs in different regions of the intestinal tract of the rat. *J. Pharm. Sci.* **1998**, *87*, 360−366.

(15) Ansede, J. H.; Thakker, D. R. High-throughput screening for stability and inhibitory activity of compounds toward cytochrome P450-mediated metabolism. *J. Pharm. Sci.* **2004**, *93*, 239−255.

(16) Amidon, G. L.; Lennernas, H.; Shah, V. P.; Crison, J. R. A theoretical basis for a biopharmaceutic drug classification: the correlation of in vitro drug product dissolution and in vivo bioavailability. *Pharm. Res.* **1995**, *12*, 413−420.

(17) Lipka, E.; Amidon, G. L. Setting bioequivalence requirements for drug development based on preclinical data: optimizing oral drug delivery systems. *J. Controlled Release* **1999**, *62*, 41−49.

(18) Jani, P.; Halbert, G. W.; Langridge, J.; Florence, A. T. The uptake and translocation of latex nanospheres and microspheres after oral administration to rats. *J. Pharm. Pharmacol.* **1989**, *41*, 809−812.

(19) Hodges, G. M.; Carr, E. A.; Hazzard, R. A.; Carr, K. E. Uptake and translocation of microparticles in small intestine. Morphology and quantification of particle distribution. *Dig. Dis. Sci.* **1995**, *40*, 967−975.

(20) Chen, H.; Langer, R. Oral particulate delivery: status and future trends. *Adv. Drug Delivery Rev.* **1998**, *34*, 339−350.

(21) Kraehenbuhl, J. P.; Neutra, M. R. Epithelial M cells: differentiation and function. *Annu. Rev. Cell Dev. Biol.* **2000**, *16*, 301−332.

(22) Eldridge, J. H.; Meulbroek, J. A.; Staas, J. K.; Tice, T. R.; Gilley, R. M. Vaccine-containing biodegradable microspheres specifically enter the gut-associated lymphoid tissue following oral administration and induce a disseminated mucosal immune response. *Adv. Exp. Med. Biol.* **1989**, *251*, 191−202.

(23) Desai, M. P.; Labhasetwar, V.; Amidon, G. L.; Levy, R. J. Gastrointestinal uptake of biodegradable microparticles: effect of particle size. *Pharm. Res.* **1996**, *13*, 1838−1845.

(24) Dressman, J. B.; Reppas, C. In vitro−in vivo correlations for lipophilic, poorly water-soluble drugs. *Eur. J. Pharm. Sci.* **2000**, *11* (Suppl. 2), S73−S80.

(25) Kostewicz, E. S.; Brauns, U.; Becker, R.; Dressman, J. B. Forecasting the oral absorption behavior of poorly soluble weak bases using solubility and dissolution studies in biorelevant media. *Pharm. Res.* **2002**, *19*, 345−349.

(26) Charman, W. N. A.; Stella, V. J. Estimating the maximal potential for intestinal lymphatic transport of lipophilic drug molecules. *Int. J. Pharm.* **1986**, *34*, 175−178.

(27) Charman, W. N. A., Stella, V. J., Eds. *Lymphatic Transport of Drugs*; CRC Press: Boca Raton, FL, 1992.

(28) Ikomi, F.; Hanna, G. K.; Schmid-Schonbein, G. W. Size- and surface-dependent uptake of colloid particles into the lymphatic system. *Lymphology* **1999**, *32*, 90−102.

(29) Kohlstaedt, L. A.; Wang, J.; Friedman, J. M.; Rice, P. A.; Steitz, T. A. Crystal structure at 3.5 Å resolution of HIV-1 reverse transcriptase complexed with an inhibitor. *Science* **1992**, *256*, 1783−1790.

(30) Ding, J.; Das, K.; Moereels, H.; Koymans, L.; Andries, K.; Janssen, P. A.; Hughes, S. H.; Arnold, E. Structure of HIV-1 RT/TIBO R 86183 complex reveals similarity in the binding of diverse nonnucleoside inhibitors. *Nat. Struct. Biol.* **1995**, *2*, 407−415.

(31) Ren, J.; Esnouf, R.; Garman, E.; Somers, D.; Ross, C.; Kirby, I.; Keeling, J.; Darby, G.; Jones, Y.; Stuart, D.; et al. High resolution structures of HIV-1 RT from four RT-inhibitor complexes. *Nat. Struct. Biol.* **1995**, *2*, 293−302.

(32) Das, K.; Clark, A. D., Jr.; Lewi, P. J.; Heeres, J.; de Jonge, M. R.; Koymans, L. M.; Vinkers, H. M.; Daeyaert, F.; Ludovici, D. W.; Kukla, M. J.; De Corte, B.; Kavash, R. W.; Ho, C. Y.; Ye, H.; Lichtenstein, M. A.; Andries, K.; Pauwels, R.; de Bethune, M. P.; Boyer, P. L.; Clark, P.; Hughes, S. H.; Janssen, P. A. J.; Arnold, E. Roles of conformational and positional adaptability in structure-based design of TMC125-R165335 (etravirine) and related non-nucleoside reverse transcriptase inhibitors that are highly potent and effective against wild-type and drug-resistant HIV-1 variants. *J. Med. Chem.* **2004**, *47*, 2550−2560.

(33) Janssen, P. A. J.; Lewi, P.; Arnold, E.; Daeyaert, F.; de Jonge, M.; Heeres, J.; Koymans, L.; Vinkers, H. M.; Guillemont, J.; Pasquier, E.; Kukla, M. J.; Ludovici, D. W.; Andries, K.; de Bethune, M. P.; Pauwels, R.; Das, K.; Clark, A.; Frenkel, Y. V.; Hughes, S. H.; Medaer, B.; De Knaep, F.; Bohets, H.; De Clerck, F.; Lampo, A.; Williams, P.; Stoffels, P. In search of a novel anti-HIV drug: Multidisciplinary coordination in the discovery of 4-[[4-[[4-[(1*E*)-2-cyanoethenyl]-2,6-dimethylphenyl]amino]-2-pyrimidinyl]amino]benzonitrile (R278474, Rilpivirine). *J. Med. Chem.*, in press.

(34) Ludovici, D. W.; Kavash, R. W.; Kukla, M. J.; Ho, C. Y.; Ye, H.; De Corte, B. L.; Andries, K.; de Bethune, M. P.; Azijn, H.; Pauwels, R.; Moereels, H. E.; Heeres, J.; Koymans, L. M.; de Jonge, M. R.; Van Aken, K. J.; Daeyaert, F. F.; Lewi, P. J.; Das, K.; Arnold, E.; Janssen, P. A. Evolution of anti-HIV drug candidates. Part 2: Diaryltriazine (DATA) analogues. *Bioorg. Med. Chem. Lett.* **2001**, *11*, 2229−2234.

(35) Ludovici, D. W.; De Corte, B. L.; Kukla, M. J.; Ye, H.; Ho, C. Y.; Lichtenstein, M. A.; Kavash, R. W.; Andries, K.; de Bethune, M. P.; Azijn, H.; Pauwels, R.; Lewi, P. J.; Heeres, J.; Koymans, L. M.; de Jonge, M. R.; Van Aken, K. J.; Daeyaert, F. F.; Das, K.; Arnold, E.; Janssen, P. A. Evolution of anti-HIV drug candidates. Part 3: Diarylpyrimidine (DAPY) analogues. *Bioorg. Med. Chem. Lett.* **2001**, *11*, 2235−2239.

(36) Sankatsing, S. U.; Weverling, G. J.; Peeters, M.; van't Klooster, G.; Gruzdev, B.; Rakhmanova, A.; Danner, S. A.; Jurriaans, S.; Prins, J. M.; Lange, J. M. TMC125 exerts similar initial antiviral potency as a five-drug, triple class antiretroviral regimen. *AIDS* **2003**, *17*, 2623−2627.

(37) Gruzdev, B.; Rakhmanova, A.; Doubovskaya, E.; Yakovlev, A.; Peeters, M.; Rinehart, A.; de Dier, K.; Baede-Van Dijk, P.; Parys, W.; van't Klooster, G. A randomized, double-blind, placebo-controlled trial of TMC125 as 7-day monotherapy in antiretroviral naive, HIV-1 infected subjects. *AIDS* **2003**, *17*, 2487−2494.

(38) Andries, K.; Azijn, H.; Thielemans, T.; Ludovici, D.; Kukla, M.; Heeres, J.; Janssen, P.; De Corte, B.; Vingerhoets, J.; Pauwels, R.; de Bethune, M. P. TMC125, a novel next-generation non-

nucleoside reverse transcriptase inhibitor active against non-nucleoside reverse transcriptase inhibitor-resistant human immunodeficiency virus type 1. *Antimicrob. Agents Chemother.* **2004**, *48*, 4680−4686.
(39) Lewi, P.; Arnold, E.; Andries, K.; Bohets, H.; Borghys, H.; Clark, A.; Daeyaert, F.; Das, K.; de Bethune, M. P.; de Jonge, M.; Heeres, J.; Koymans, L.; Leempoels, J.; Peeters, J.; Timmerman, P.; Van den Broeck, W.; Vanhoutte, F.; Van't Klooster, G.; Vinkers, M.; Volovik, Y.; Janssen, P. A. Correlations between factors determining the pharmacokinetics and antiviral activity of HIV-1 non-nucleoside reverse transcriptase inhibitors of the diaryltriazine and diarylpyrimidine classes of compounds. *Drugs R&D* **2004**, *5*, 245−257.
(40) Raschke, T. M.; Tsai, J.; Levitt, M. Quantification of the hydrophobic interaction by simulations of the aggregation of small hydrophobic solutes in water. *Proc. Natl. Acad. Sci. U.S.A.* **2001**, *98*, 5965−5969.
(41) *DynaPro-MS800*, version 5.26.60; Protein Solutions, Inc.: Lakewood, NJ, 2000.
(42) *JMP Statistical Discovery Software*, version 3.1; SAS Institute Inc.: Cary, NC, 1995.
(43) Regev, O.; Zana, R. Aggregation behavior of tyloxapol, a nonionic surfactant oligomer, in aqueous solution. *J. Colloid Interface Sci.* **1999**, *210*, 8−17.
(44) Pauwels, R.; Balzarini, J.; Baba, M.; Snoeck, R.; Schols, D.; Herdewijn, P.; Desmyter, J.; De Clercq, E. Rapid and automated tetrazolium-based colorimetric assay for the detection of anti-HIV compounds. *J. Virol. Methods* **1988**, *20*, 309−321.
(45) Neuhoff, S.; Ungell, A. L.; Zamora, I.; Artursson, P. pH-dependent bidirectional transport of weakly basic drugs across Caco-2 monolayers: implications for drug−drug interactions. *Pharm. Res.* **2003**, *20*, 1141−1148.
(46) Kostewicz, E. S.; Wunderlich, M.; Brauns, U.; Becker, R.; Bock, T.; Dressman, J. B. Predicting the precipitation of poorly soluble weak bases upon entry in the small intestine. *J. Pharm. Pharmacol.* **2004**, *56*, 43−51.
(47) McGovern, S. L.; Caselli, E.; Grigorieff, N.; Shoichet, B. K. A common mechanism underlying promiscuous inhibitors from virtual and high-throughput screening. *J. Med. Chem.* **2002**, *45*, 1712−1722.
(48) McGovern, S. L.; Helfand, B. T.; Feng, B.; Shoichet, B. K. A specific mechanism of nonspecific inhibition. *J. Med. Chem.* **2003**, *46*, 4265−4272.
(49) Pacheco, L. F.; Carmona-Ribeiro, A. M. Effects of synthetic lipids on solubilization and colloid stability of hydrophobic drugs. *J. Colloid Interface Sci.* **2003**, *258*, 146−154.
(50) Seidler, J.; McGovern, S. L.; Doman, T. N.; Shoichet, B. K. Identification and prediction of promiscuous aggregating inhibitors among known drugs. *J. Med. Chem.* **2003**, *46*, 4477−4486.
(51) Forssell, H. Gastric mucosal defence mechanisms: a brief review. *Scand. J. Gastroenterol., Suppl.* **1988**, *155*, 23−28.
(52) Camilleri, M.; Colemont, L. J.; Phillips, S. F.; Brown, M. L.; Thomforde, G. M.; Chapman, N.; Zinsmeister, A. R. Human gastric emptying and colonic filling of solids characterized by a new method. *Am. J. Physiol.* **1989**, *257*, G284−G290.
(53) Waterman, K. C.; Sutton, S. C. A computational model for particle size influence on drug absorption during controlled-release colonic delivery. *J. Controlled Release* **2003**, *86*, 293−304.

JM049439I